Topics in Catalysis Vols. 42–43, May 2007 (© 2007)
DOI: 10.1007/s11244-007-0151-9

Role and distribution of different Ba-containing phases in supported Pt–Ba NSR catalysts

M. Piacentini, M. Maciejewski, and A. Baiker*

Department of Chemistry and Applied Biosciences, Institute of Chemical and Bioengineering, ETH-Zurich, Hönggerberg, HCI, 8093 Zurich, Switzerland

Pt–Ba/MeO (where MeO = Al_2O_3, CeO_2, SiO_2 and ZrO_2) NO_x storage-reduction catalysts with Ba-loading varying from 0 wt.% to 28 wt.% were investigated concerning stability of Ba phases and NO_x storage-reduction efficiency. For Pt–Ba/Al_2O_3 three different Ba-containing phases with different thermal stability are distinguished based on their interaction with the support. The relative concentration of these phases varies with the Ba-loading and NO_x storage tests indicated that the $BaCO_3$ phase decomposing between 400 °C and 800 °C (LT-$BaCO_3$) is the most efficient Ba containing phase for NO_x storage. Similar investigations of Pt–Ba catalysts supported on CeO_2, SiO_2 and ZrO_2 showed that the relative amount of LT-$BaCO_3$ phase depends also on the support material. NO_x storage measurements confirmed a correlation between the concentration of LT-$BaCO_3$ and NO_x storage efficiency. Basicity and textural properties of the support are identified as crucial parameters for efficient NO_x storage catalysts.

KEY WORDS: NO_x storage-reduction catalysts; Pt–Ba/ceria; Pt–Ba/zirconia; Pt–Ba/silica; Pt–Ba/alumina; NO_x storage efficiency; effect of Ba-loading; stability of barium carbonates.

1. Introduction

The introduction of more efficient combustion engines operating under lean conditions stimulated the development of new catalysts for NO_x pollution control. In 1995 Toyota successfully proposed NO_x storage-reduction (NSR) catalysts for dynamic NO_x control [1]. The NSR process is based on storage of nitrogen oxides under lean conditions over an alkaline or alkaline-earth component (i.e. $BaCO_3$ or BaO) in the form of nitrates which are then reduced to nitrogen during a short fuel rich period [2]. The original catalyst formulation, Pt–Ba/Al_2O_3 (Ba-loading varies from 8 wt.% to 20 wt.%), prepared by wet impregnation of an alumina support with aqueous solutions of barium and platinum precursors has been extensively studied [3,4].

Recent studies evidenced the existence of different NO_x storage active sites [5–8]. Detailed characterization of Ba-containing species on the support indicated that, depending on their interaction with the support [9,10], they posses different stability and NO_x storage efficiency [11,12].

Al_2O_3, CeO_2, ZrO_2, Ce–Zr-oxides and SiO_2 are widely used in the control of combustion pollutants [13–21] and in our studies we specifically addressed the comparison of these oxides as supports in Pt–Ba based NO_x storage-reduction catalysts. Preliminary results on Pt–Ba catalysts supported on different oxides indicated different NO_x storage behavior depending on the support [9].

* To whom correspondence should be addressed.
E-mail: baiker@chem.ethz.ch

Here we first revisit the influence of the support-active Ba-phase interaction on the relative distribution of Ba-containing species and correlate it with the NO_x storage activity of Pt–Ba/Al_2O_3 catalysts. Then, we extend the study to corresponding Pt–Ba catalysts supported on CeO_2, SiO_2 and ZrO_2, and analyze how the distribution of Ba-containing species and the related NO_x storage activity are affected by the properties of support materials.

2. Experimental

Pt–Ba supported NO_x storage catalysts with different Ba-loading (4.5–28 wt.%) were prepared by incipient wetness method [10,11]. First, 1 wt.% of Pt was loaded by impregnation with $Pt(NH_3)_2(NO_2)_2$ solutions onto the supports calcined at 500 °C in air. The Pt/support samples were then dried at 80 °C for 12 h, calcined at 500 °C for 5 h in air, impregnated with differently concentrated $Ba(CH_3COO)_2$ solutions and then dried again at 80 °C for 12 h. The samples are designated as Pt–Ba(x), where x denotes the weight % of Ba in the sample, e.g. Pt–Ba(22). Dried samples were calcined *in situ* prior to each experiment in 20 vol.% O_2/He at 500 °C, and then allowed to cool to reaction temperature under controlled atmosphere.

XRD analysis was carried out on a Siemens D5000 powder X-ray diffractometer using the Cu-Kα radiation in step mode between 10 and 80° 2θ with a step of 0.01° and 2 s step^{-1}.

Thermogravimetry (TG) combined with mass spectrometry (MS) was performed on a Netzsch STA 409

1022-5528/07/0500-0055/0

thermoanalyzer which was connected to a valve device enabling pulse thermal analysis (Pulse TA®). This set-up [22] allows the injection of controlled amounts (0.5–5 mL) of probe gas into a carrier gas stream (here fixed at 50 $Ncm^3\ min^{-1}$) flowing through the thermoanalyzer. The composition of the gas phase was monitored by a ThermoStar Pfeiffer Vacuum GSD 301 O1 mass spectrometer, which was connected to the thermoanalyzer by a heated (ca. 200 °C) stainless steel capillary.

Temperature-programmed reaction-desorption (TPRD) experiments were carried out in He with a heating rate of 10 °C min^{-1}. NO_x storage tests were performed at 300 °C in a 5 vol.% O_2/He atmosphere, with repeated 1 cm^3 NO pulses injected into a carrier gas stream till saturation of active sites (maximal mass uptake) was reached.

3. Results and discussion

3.1. Influence of Ba-loading on thermal stability and NO_x storage efficiency of Pt–Ba/Al_2O_3 catalyst

Alumina-supported Pt–Ba catalysts with different Ba-loadings were investigated with respect to the stability and NO_x storage activity of different Ba-containing species formed during calcination of barium precursor $Ba(Ac)_2$.

The XRD analysis of freshly calcined samples indicated the presence of crystalline $BaCO_3$ for Ba loadings higher than 16.7 wt.% (figure 1). Both, the major, orthorhombic (whiterite) and the monoclinic phases were present, the latter being metastable and progressively disappearing with time [10,23–25].

Evaluation of different $BaCO_3$ phases formed during decomposition of $Ba(Ac)_2$ was achieved through quantification of evolved CO_2 according to the stoichiometry of the reaction $BaCO_3 \rightarrow BaO + CO_2$ during TPRD experiments (figure 2). Three types of $BaCO_3$ with different thermal stability resulting from their different interaction with the support have been detected: (i) very unstable $BaCO_3$ in intimate contact with the alumina, decomposing at temperature lower than 500 °C and forming BaO, (ii) *Low-Temperature barium carbonate* (LT-$BaCO_3$) being in direct contact with the BaO layer and decomposing between 400 °C and 800 °C, and (iii) bulk-like, *High-Temperature barium carbonate* (HT-$BaCO_3$) decomposing at temperatures higher than 800 °C and being present in the form of larger aggregates that are less affected by the support influence.

The distribution of these $BaCO_3$ phases depends on the Ba-loading (figure 3) and on the nature of the support. The influence of the support is most prominent at low loadings, while the progressive growth of Ba-containing domains, at higher Ba-loading (> ca. 16.7 wt.%) does not contribute anymore to the Ba/support interface.

Catalysts calcined at 500 °C, containing LT- and HT-$BaCO_3$, were exposed to NO pulses in 5 vol.% O_2/He atmosphere till saturation of the active storage sites was achieved. Assuming that NO_x species are stored as nitrates allowed to quantify the amount of NO stored by TPRD of NO_x saturated catalysts and to derive the fraction of active Ba [9,24,26]. The NO_x storage efficiency is presented in figure 4 in terms of fraction of Ba involved in the NO_x storage process versus the total Ba loaded.

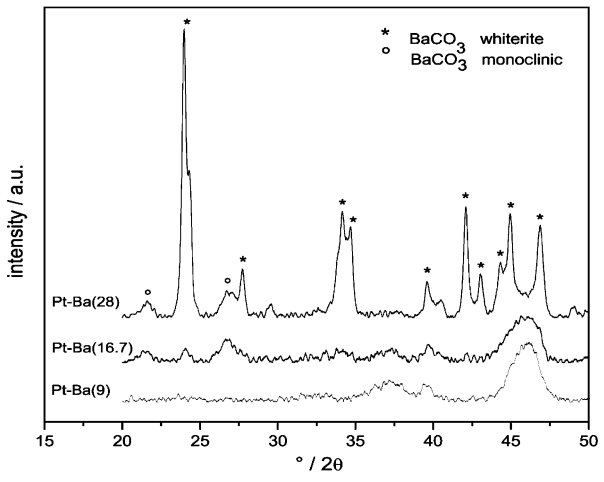

Figure 1. XRD patterns of Pt/Al_2O_3 loaded with $Ba(Ac)_2$ after calcination in 20 vol.% O_2/He up to 500 °C. Crystalline monoclinic and orthorhombic (whiterite) $BaCO_3$ could be detected for Ba loadings higher than ca. 16 wt.%. Unlabeled reflections correspond to γ-Al_2O_3. XRD analysis was carried out with freshly calcined samples, avoiding long term ambient atmosphere exposure.

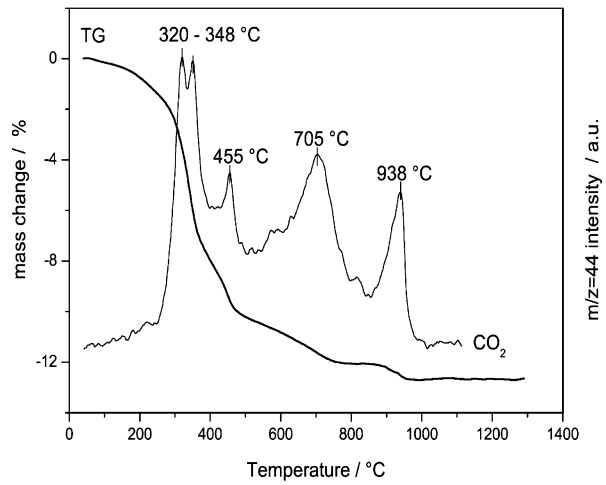

Figure 2. TPRD in He atmosphere of Pt–Ba(22)/Al_2O_3 catalyst. Thermogravimetric (TG) curve and mass spectrometric signal $m/z = 44$ tracing the mass changes and CO_2 evolution resulting from the decomposition of $Ba(Ac)_2$ followed by the decomposition of formed $BaCO_3$.

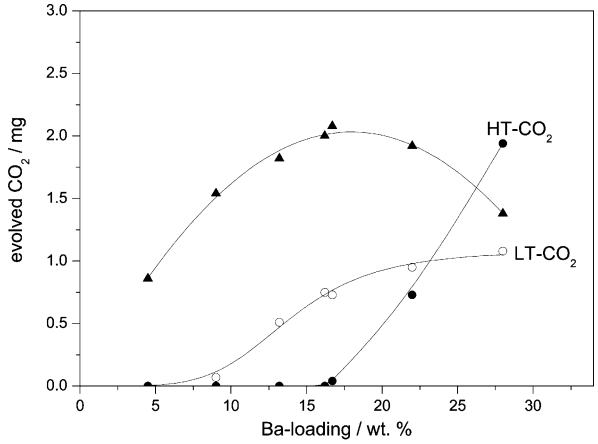

Figure 3. Influence of Ba-loading on amount of CO_2 evolved during decomposition of $BaCO_3$ phases, formed during calcination of $Ba(Ac)_2$ deposited on Pt/Al_2O_3, (▲) up to 400 °C; (○) between 400 °C and 800 °C (Low Temperature $BaCO_3$); (●) at temperatures above 800 °C (High Temperature $BaCO_3$).

The volcano shaped curve clearly indicates that the storage efficiency is affected by the Ba-loading [27], particularly a correlation can be found with the relative concentration of LT- and HT-$BaCO_3$ phases. At low Ba-loading the NO_x storage efficiency curve grows parallel with the increase of the concentration of LT-$BaCO_3$, indicating that this phase contributes mainly to the storage activity. At higher Ba-loading, once the HT-$BaCO_3$ phase starts to form, the NO_x storage efficiency decreases, indicating that HT-$BaCO_3$ shows a poor NO_x storage activity, comparable to that of bulk $BaCO_3$ (not shown) and is affected by diffusional limitation [28–30].

3.2. *Influence of support on Ba-containing species stability and NO_x storage efficiency*

Series of Pt–Ba supported on CeO_2 SiO_2 and ZrO_2 were prepared varying the Ba content from 4.5 wt.% to 28 wt.%. Depending on the support, calcination of the samples loaded with $Ba(Ac)_2$ precursor resulted in different relative amount of barium carbonate. Figure 5 shows the influence of the support and Ba-loading on the relative amount of $BaCO_3$ formed. SiO_2 supported $Ba(Ac)_2$ decomposed completely to BaO and only a minimal amount of carbonates formed by $Ba(Ac)_2$ decomposition is stable at very high Ba-loading. In contrast, on CeO_2 and ZrO_2, a substantial amount of stable carbonates formed during $Ba(Ac)_2$ decomposition. The distribution of LT- and HT-$BaCO_3$ phases as a function of Ba-loading and kind of support is presented in figure 6A and B, respectively. Note that the concentration of LT-$BaCO_3$ at low Ba-loading depends strongly on the support (figure 6A). CeO_2 and ZrO_2 seem to better stabilize the carbonates formed during precursor decomposition than Al_2O_3 which results in significantly higher concentration of LT-$BaCO_3$ on these supports at lower Ba-loadings. On the other hand, the concentration of HT-$BaCO_3$ is rather independent of the kind of support, even if the higher stability of $BaCO_3$ in CeO_2 and ZrO_2 samples leads to the formation of bulk-like carbonates at significantly lower Ba loadings (figure 6B).

The ability of the different supports to stabilize the carbonates formed from the $Ba(Ac)_2$ decomposition decreases in the order $CeO_2 \cong ZrO_2 > Al_2O_3 > SiO_2$. Interestingly, according to Martin and Duprez [31] the basicity order of the investigated supports in terms of CO_2 chemisorption is similar: $CeO_2 > ZrO_2 > > Al_2O_3 > SiO_2$ indicating that CO_2 chemisorbs best on CeO_2. This suggests that the observed effect of the supports on the stability of the Ba-containing species can be traced to their different basicity. CO_2 chemisorption is

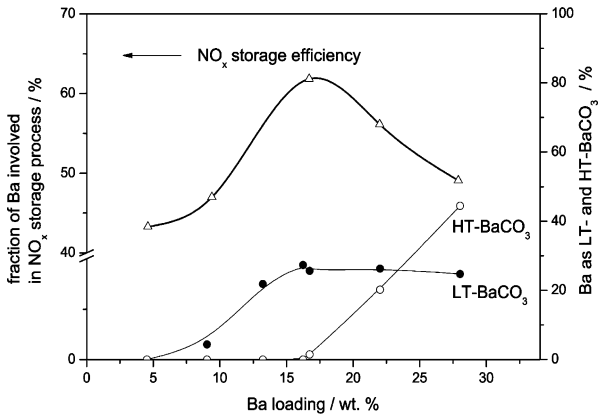

Figure 4. NO_x storage efficiency as a function of Ba-loading and $BaCO_3$ distribution. Note that the volcano shaped efficiency curve can be addressed to the concentrations of more active LT-$BaCO_3$ and less active HT-$BaCO_3$ phase.

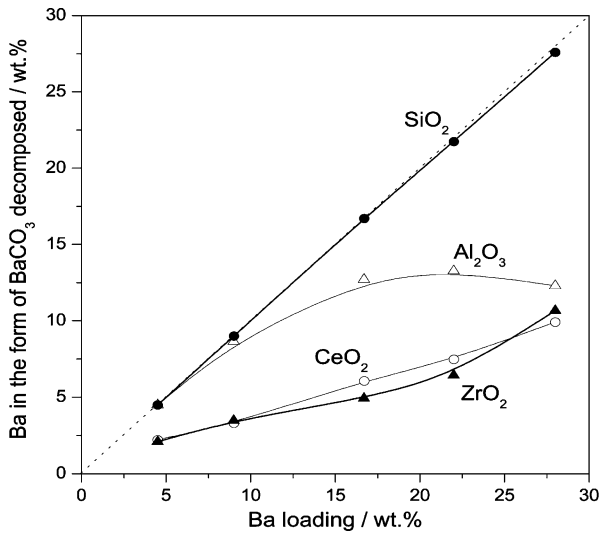

Figure 5. Influence of the support and Ba-loading on the stability of $BaCO_3$ formed during decomposition of $Ba(Ac)_2$ supported on different oxides. In silica supported samples $BaCO_3$ fully decomposes during calcination.

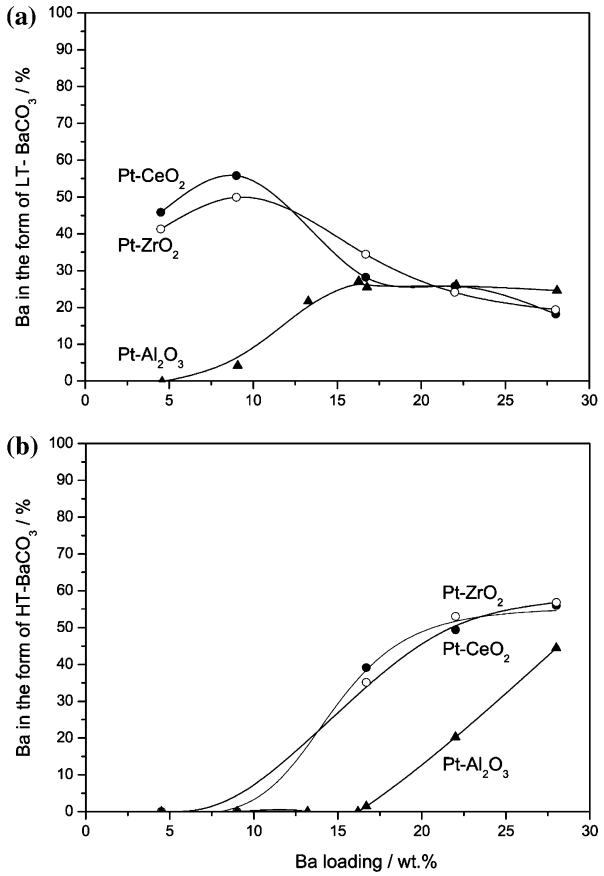

Figure 6. Distribution of $BaCO_3$ phases over different supports as a function of Ba-loading: (**a**) LT-$BaCO_3$ and (**b**) HT-$BaCO_3$.

favored on basic supports, resulting in the formation of stable $BaCO_3$. The ability of surface active sites to interact with CO_2 species affording the formation of stable carbonates [32] is thus a major factor for explaining the influence of the support on the distribution of Ba-containing phases. CO_2 strongly chemisorbed on CeO_2 and ZrO_2 is in close contact with BaO, which results in formation of the $BaCO_3$ phases. In contrast, when CO_2 does not, or only weakly chemisorbs on the support, as in the case of SiO_2, $BaCO_3$ formed during $Ba(Ac)_2$ decomposition is unstable and decomposes to BaO at low temperature. Only at high Ba-loading the formed BaO covers the support allowing CO_2 chemisorption and, in turn, the formation of $BaCO_3$ phases.

Although, silica is an unfavorable support to stabilize barium carbonate its intrinsically high surface area could be advantageous when covered with basic oxides, like CeO_2 and ZrO_2, which favor the formation of the most active LT-$BaCO_3$.

NO_x storage tests confirmed the correlation between the presence of active LT-$BaCO_3$ and NO_x storage efficiency (figure 7). At low Ba-loading CeO_2 and ZrO_2 exhibit a higher concentration of Ba active sites consistently with their higher concentration of LT-$BaCO_3$, whereas at higher Ba-loading the decreasing support

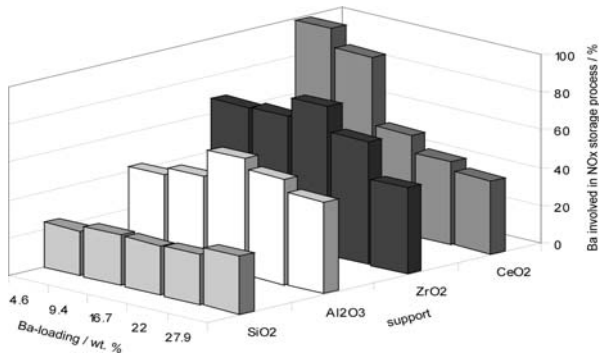

Figure 7. NO_x storage efficiency expressed in terms of percentage of Ba active in NO_x storage: influence of the Ba-loading and the support.

effect somehow equalizes the storage performance of Al_2O_3, CeO_2 and ZrO_2 supported catalysts. However, morphological differences of the supports will also affect the storage performance. The almost complete absence of carbonates over SiO_2 renders silica an unsuitable interface for accommodating barium carbonate.

4. Conclusions

In standard NSR Pt–Ba/Al_2O_3 catalysts with 1 wt.% of Pt and Ba-loading varying from 4.5 wt.% to 28 wt.% three different Ba-containing phases can be distinguished in calcined catalysts: (i) very unstable $BaCO_3$ decomposing to BaO at $T < 500$ °C, (ii) LT-$BaCO_3$ being in intimate contact with BaO and decomposing between 400 °C and 800 °C, and (iii) high temperature $BaCO_3$ (HT-$BaCO_3$) decomposing at $T > 800$ °C. Relative concentrations of these phases depend on the Ba-loading. The NO_x storage efficiency is strongly related to the concentration of the LT-$BaCO_3$ phase. Highest population density of active Ba sites is achieved at ca. 16 wt.% of Ba.

Investigations of Pt–Ba catalysts supported on CeO_2, SiO_2 and ZrO_2 revealed that the relative distribution of the Ba-containing phases depends on the chemical and structural properties of the supports. Basic supports as CeO_2 and ZrO_2 show highest relative concentration of LT-$BaCO_3$ at low Ba-loading due to their ability to stabilize carbonates. As a consequence, CeO_2 and ZrO_2 supported catalysts are the most efficient catalysts at low Ba-loading. SiO_2 supported catalysts show poor NO_x storage capacity due to very low stability of barium carbonate on this support. Consequently, the barium component should not be located at the silica interface in silica-containing storage catalysts.

References

[1] N. Miyoshi, S. Matsumoto, K. Katoh, T. Tanaka, J. Harada, N. Takahashi, K. Yokota, M. Sugiura and K. Kasahara, SAE Tech. Paper 950809 (1995).

[2] N. Takahashi, H. Shinjoh, T. Iijima, T. Suzuki, K. Yamazaki, K. Yokota, H. Suzuki, N. Miyoshi, S. Matsumoto, T. Tanizawa, T. Tanaka, S. Tateishi and K. Kasahara, Catal. Today 27 (1996) 63.
[3] W.S. Epling, L.E. Campbell, A. Yezerets, N.W. Currier and J.E. Parks, Catal. Rev. 46 (2004) 163.
[4] Z. Liu and S.I. Woo, Catal. Rev. 48 (2006) 43.
[5] W.S. Epling, J.E. Parks, G.C. Campbell, A. Yezerets, N.W. Currier and L.E. Campbell, Catal. Today 96 (2004) 21.
[6] P.T. Fanson, M.R. Horton, W.N. Delgass and J. Lauterbach, Appl. Catal. B 46 (2003) 393.
[7] J. Szanyi, J.H. Kwak, D.H. Kim, S.D. Burton and C.H.F. Peden, J. Phys. Chem. B 109 (2005) 27.
[8] X. Chen, J. Schwank, J. Li, W.F. Schneider, J. Goralski, T. Christian and P.J. Schmitz, Appl. Catal. B 61 (2005) 189.
[9] M. Piacentini, M. Maciejewski, T. Burgi and A. Baiker, Top. Catal. 30–31 (2004) 71.
[10] M. Piacentini, M. Maciejewski and A. Baiker, Appl. Catal. B 65 (2006) 157.
[11] M. Piacentini, M. Maciejewski and A. Baiker, Appl. Catal. B 59 (2005) 187.
[12] M. Piacentini, M. Maciejewski and A. Baiker, Appl. Catal. B 60 (2005) 265.
[13] J. Kaspar, P. Fornasiero and N. Hickey, Catal. Today 77 (2003) 419.
[14] M. Fernandez-Garcia, A. Martinez-Arias, A. Iglesias-Juez, A.B. Hungria, J.A. Anderson, J.C. Conesa and J. Soria, J. Catal. 214 (2003) 220.
[15] C.M. Ho, J.C. Yu, X.C. Wang, S.Y. Lai and Y.F. Qiu, J. Mat. Chem. 15 (2005) 2193.
[16] P. Svedberg, E. Jobson, S. Erkfeldt, B. Andersson, M. Larsson and M. Skoglundh, Top. Catal. 30–31 (2004) 199.
[17] V.G. Milt, C.A. Querini, E.E. Miro and M.A. Ulla, J. Catal. 220 (2003) 424.
[18] M.L. Pisarello, V. Milt, M.A. Peralta, C.A. Querini and E.E. Miro, Catal. Today 75 (2002) 465.
[19] S. Benard, L. Retailleau, F. Gaillard, P. Vernoux and A. Giroir-Fendler, Appl. Catal. B 55 (2005) 11.
[20] M. Eberhardt, R. Riedel, U. Göbel, J. Theis and E.S. Lox, Top. Catal. 30–31 (2004) 135.
[21] M. Casapu, J.D. Grunwaldt, M. Maciejewski, M. Wittrock, U. Göbel and A. Baiker, Appl. Catal. B 63 (2006) 232.
[22] M. Maciejewski, C.A. Müller, R. Tschan, W.D. Emmerich and A. Baiker, Thermochim. Acta 295 (1997) 167.
[23] R. Strobel, M. Maciejewski, S.E. Pratsinis and A. Baiker, Thermochim. Acta, 445 (2006) 23.
[24] L. Lietti, P. Forzatti, I. Nova and E. Tronconi, J. Catal. 204 (2001) 175.
[25] F. Prinetto, G. Ghiotti, I. Nova, L. Lietti, E. Tronconi and P. Forzatti, J. Phys. Chem. B 105 (2001) 12732.
[26] I. Nova, L. Castoldi, F. Prinetto, V. Dal Santo, L. Lietti, E. Tronconi, P. Forzatti, G. Ghiotti, R. Psaro and S. Recchia, Top. Catal. 30/31 (2004) 181.
[27] L. Castoldi, I. Nova, L. Lietti and P. Forzatti, Catal. Today 96 (2004) 43.
[28] U. Tuttlies, V. Schmeisser and G. Eigenberger, Chem. Eng. Sci. 59 (2004) 4731.
[29] R.L. Muncrief, P. Khanna, K.S. Kabin and M.P. Harold, Catal. Today 98 (2004) 393.
[30] L. Olsson, 7th DOE Crosscut Workshop on Lean Emissions Reduction Simulation, CLEERS Detroit (MI) 2004.
[31] D. Martin and D. Duprez, J. Mol. Catal. A 118 (1997) 113.
[32] G. Busca and V. Lorenzelli, Mat. Chem. 7 (1982) 89.